PAPER

Modelling radiation emission in the transition from the classical to the quantum regime

IOP Publishing Plasma Physics and Controlled Fusion

Plasma Phys. Control. Fusion **58** (2016) 014035 (8pp) doi:10.1088/0741-3335/58/1/014035

Modelling radiation emission in the transition from the classical to the quantum regime

J L Martins[1], M Vranic[1], T Grismayer[1], J Vieira[1], R A Fonseca[1,2] and L O Silva[1]

[1] GoLP/Instituto de Plasmas e Fusão Nuclear, Instituto Superior Técnico, Universidade de Lisboa, 1049-001 Lisbon, Portugal

[2] DCTI/ISCTE Instituto Universitário de Lisboa, 1649-026 Lisboa, Portugal

E-mail: jlmartins@ist.utl.pt

Received 20 July 2015, revised 28 September 2015
Accepted for publication 14 October 2015
Published 26 November 2015

Abstract

An emissivity formula is derived using the generalised Fermi–Weizäcker–Williams method of virtual photons, which accounts for the recoil the charged particle experiences as it emits radiation. It is found that through this derivation the result obtained by Sokolov *et al* using QED perturbation theory is recovered. The corrected emissivity formula is applied to nonlinear Thomson scattering scenarios in the transition from the classical to the quantum regime for small values of the nonlinear quantum parameter χ. In addition, signatures of the quantum corrections are identified and explored.

Keywords: radiation, radiation damping, quantum

1. Introduction

Increases in the available laser power and high-energy electron beams (reaching a few GeV; for e.g. [1–3]) obtained with plasma-based accelerators allow us to reach new regimes in laser-beam scattering in all-optical configurations [4–6]. The scattering of high-intensity lasers on relativistic beams can lead to the strong emission of radiation, accompanied by the loss of energy by the electrons. Depending on the energy of the particle and the strength of the field, the energy loss by the electron during emission may or may not be comparable to its own energy. If the emitted photon energy is negligible compared to the electron energy, the scattering is purely classical; in the other case, the electron momentum changes during emission. This recoil is a quantum effect and, depending on its importance relative to the energy of the electron, can change its trajectory in a smooth or stochastic manner. The importance of this and other quantum effects on radiation emission can be parameterised by:

$$\chi = \frac{|F^{\mu\nu} p_\nu|}{E_{\text{crit}} mc}, \tag{1}$$

which is approximately equal to the ratio between the field amplitude in the rest frame of the electron and the Schwinger critical field for very relativistic electrons, and [17]

$$\rho = \frac{\hbar k^\nu p_\nu}{m^2 c^2}, \tag{2}$$

which gives the ratio of the laser photon energy in the rest frame of the electron to its rest energy. Here, $E_{\text{crit}} = m^2c^3/(e\hbar)$ is the Schwinger critical field, $F^{\mu\nu}$ is the electromagnetic wave field-strength tensor, p_ν is the electron momentum four-vector and k^ν is the emitted photon momentum four-vector.

In the presence of laser-fields, the normalised vector potential of the laser, given by $a_0 = eA_0/(m_e c^2)$, describes the nature of the dynamics of the electron. For low-intensity lasers, $a_0 \ll 1$ to $a_0 \leqslant 1$, quantum effects can still occur but their importance is measured by the parameter ρ [17]. In the opposite case, for very intense lasers, $a_0 \gg 1$, the electron dynamics in the laser is nonlinear and radiation is emitted at multiple harmonics (nonlinear Thomson [8, 9]/Compton [10, 11] scattering). In this regime, the importance of quantum effects is determined by the nonlinear quantum parameter χ.

When $\chi \lesssim 1$ emission occurs through Compton scattering and, as the emitted energy becomes comparable to the electron energy, the trajectory becomes stochastic; at $\chi \sim 1$ processes such as pair production become significant and at $\chi > 1$ spin effects in the radiation become non-negligible. However, for $\chi \ll 1$, the trajectory of the electron can still be described classically if one accounts for the radiation reaction force. The emission process is Thomson scattering, the classical analogue of Compton scattering. In the above paragraph, the definition for nonlinear Thomson/Compton scattering from [12] is used.

In this work, the regime of radiation emission with $\chi \ll 1$ to <1, $a_0 \gg 1$ and $\gamma \gg 1$ will be studied, where γ is the Lorentz factor of the electron. In it, radiation damping is non-negligible but can be described classically and the higher harmonics of nonlinear Thomson scattering extend to energies approaching the energy of the electron, such that the classical emissivity formula derived from the Liénard–Wiechert potentials may not be valid anymore. The question then arises of how to model radiation emission in this scenario.

Several techniques have been used, such as semi-classical calculations [13–16], QED perturbation theory [18], the introduction of functions that correct the equation of motion and the radiated power/spectrum [18–20], and Monte-Carlo methods, either based on the cross sections for Compton scattering [21, 22] or on the emission probability function and spectrum of synchrotron radiation combined [23–26, 27].

In this paper we show how to derive a quantum corrected emissivity formula for arbitrary observation directions using the generalised method of Fermi–Weizäcker–Williams, first developed by Lieu and Axford [29]. This formula is implemented in the post-processing radiation diagnostic code JRad [29], which will be referred to as JRad-QC when using the quantum corrected emissivity formula. It is then used to explore the changes that occur in the Thomson scattering spectrum in the transition from the classical to the weakly quantum regime ($\chi \ll 1$). In this regime, the recoil experienced by the electron is not negligible but the trajectory can still be described by the Landau and Lifshitz equation of motion, and effects such as pair production and spin effects in radiation emission are not important. For convenience, the designation quantum regime will be used in the rest of the paper, in the sense of weakly quantum regime (or in the designation of Sokolov *et al* QED-weak fields [30]). It should be noted that the transition from the classical to the (weakly) quantum regime is not sharply defined.

This paper is structured as follows: in section 1, a quantum corrected emissivity formula is derived. In section 2, comparisons are shown between the spectrum computed with this technique and the spectra obtained through a QED probabilistic approach [26] for synchrotron radiation. In section 3, we explore nonlinear Thomson scattering in the transition from the classical to the quantum regime with JRad and trajectories obtained from the integration of the equation of motion with the radiation reaction force [31]. We show that under certain conditions a unique signature of the quantum corrections is observed, which is not seen if only the radiation damping is taken into account in the trajectory. In section 4 we state the main conclusions of the paper.

2. Radiation emissivity with quantum corrections

The method of Lieu and Axford consists of an extension of the method of virtual photons (the FWW method) [28]. This method was originally applied to problems such as bremsstrahlung radiation, where the electron was considered to be in uniform motion. The application of the FWW method to scenarios such as an electron gyrating in a uniform and static magnetic field is not possible, since there is no single rest frame for the electron. Lieu and Axford proposed a method to overcome this issue [28]. Their solution relies on splitting the electron trajectory into a series of infinitesimal segments in which the electron velocity is approximately constant and therefore the method of virtual photons can be applied. They then derive the classical results of synchrotron radiation by determining the Thomson scattering spectrum in this series of instantaneous rest frames, transforming the emissivities back to the laboratory and then adding them coherently. Quantum corrections associated with the recoil of the electron during the emission process are added by replacing the Thomson scattering cross section by the Compton cross section and ω by ω/η, where η is the Compton shift. Although Lieu and Axford have extended their work to three-dimensional scenarios and inhomogeneous magnetic fields [32], their 3D emissivity formula only reduces (in the absence of quantum corrections) to the general classical emissivity result for certain angles of observation.

In the following, it is shown that by introducing an additional generalisation to the method of Lieu and Axford, it is possible to obtain a quantum corrected emissivity formula which reduces to the three-dimensional classical emissivity (in the far field) within the limit of a negligible Compton shift for arbitrary directions of observation. For the sake of completeness, the essential steps in the derivation are presented here; further details can be found in references [28–33].

First, the trajectory is split into infinitesimal segments. A coordinate transformation is performed in the laboratory frame such that the segment to be analysed has its beginning at the origin. A Lorentz transformation is then performed to the instantaneous rest frame of the electron for this segment. In this frame, the component of the Poynting flux for the frequency ω', $S'(\omega')$ is given by:

$$S'(\omega') = c\left|\frac{1}{2\pi}\int \mathbf{E}' e^{i\omega' t'} dt'\right|^2, \tag{3}$$

where c is the velocity of light, $\mathbf{E}'$ is the incident electric field, t' is time and the primed variables refer to quantities in the instantaneous rest frame.

In this infinitesimally small segment the electron will remain non-relativistic and the electric field can be related to the electron velocity by the equation of motion $m\dot{\mathbf{v}}'_\perp = e\mathbf{E}'$, where m and e are the mass and charge of the electron, $\dot{\mathbf{v}}'_\perp$ is the acceleration of the electron and $\gamma \sim$ cte. Here, the suffix $\perp$ indicates the vector components perpendicular to the electron velocity in the laboratory frame $\boldsymbol{\beta}$. In the following calculations it is assumed that the field components in the direction of the electron momentum are negligible, i.e. that the fields the particle is subject to are approximately perpendicular to its velocity. This can also be stated in terms of a condition on

the particle acceleration, i.e. that in the infinitesimal segment under consideration $a'_{\perp} \gg a'_{\parallel}$. This is equivalent to the condition in the laboratory that $F_{\parallel} \ll \gamma F_{\perp}$, where F is the external force the particle is subject to.

Assuming that the field can be decomposed into a series of plane waves, it can be written as (for a given spectral component):

$$\mathbf{E}'_{\perp} = E'_{\perp} \exp(\mathrm{i}\omega' t' - \mathbf{k}' \cdot \mathbf{r}')\mathbf{e}_{\perp}. \tag{4}$$

If the particle moves negligibly in the wave propagation direction in the interval $\Delta t'$ and if the field changes in a time scale slower than $\Delta t'$, the time variation in $\mathbf{k}' \cdot \mathbf{r}'$ can be neglected in the integration calculation. The electric field can then be expressed in terms of the electron velocity (using the equation of motion):

$$\mathbf{E}' = \frac{m}{e}\dot{\mathbf{v}}'_{\perp} = \frac{m}{e}\mathrm{i}\omega' v'_{\perp} \exp(\mathrm{i}\omega' t')\mathbf{e}_{\perp} = \frac{m}{e}\mathrm{i}\omega'\mathbf{v}'_{\perp}, \tag{5}$$

Given the above considerations and since the interval $\Delta t'$ is considered to be infinitesimal, the integral in (3) can be taken to be approximately the integrand times the time interval:

$$\mathbf{v}'_{\perp}(t') = \frac{e}{m}\frac{\mathbf{E}'_{\perp}(t')}{\mathrm{i}\omega'}\mathbf{e}_{\perp} \Leftrightarrow \mathbf{E}'_{\perp}(t') = \frac{m}{e}\mathrm{i}\omega'\mathbf{v}'_{\perp}(t'), \tag{6}$$

where $\Delta t'$ is the time the electron takes to cross the infinitesimal segment.

The emissivity at a frequency ω' (energy radiated at a frequency ω' per unit of frequency and per unit of solid angle) in the infinitesimal segment of trajectory, $\Delta\alpha'$, is given by the product of the incident radiation flux and the Compton cross section $(\mathrm{d}\sigma'/\mathrm{d}\,\Omega')_C = [e^2/(mc^2)]^2\,\eta' \left|\boldsymbol{\epsilon}'_{\mathrm{out}} \cdot \boldsymbol{\epsilon}'_{\mathrm{in}}\right|^2$, where $\boldsymbol{\epsilon}'_{\mathrm{in}}$ and $\boldsymbol{\epsilon}'_{\mathrm{out}}$ are the polarisation vectors of the incident and outgoing photons and

$$\eta' = 1 - \frac{\hbar\omega'}{mc^2}(1 - \cos\Psi') \tag{7}$$

where Ψ' is the Compton scattering angle [28]. In the laboratory coordinates this can be expressed as:

$$\eta \simeq 1 - \frac{\hbar\omega}{\gamma mc^2} \tag{8}$$

where the approximation involves an error of order $O(1/\gamma^2)$ [28, 32]. To account for the Compton shift corrections, ω' is replaced by ω'/η' and the associated substitution [28]:

$$\Delta\alpha' \longrightarrow \Delta\alpha'\,\eta'^2 \tag{9}$$

is made, where $\Delta\alpha'$ is a contribution to the emissivity $\alpha' = \mathrm{d}^2 I/(\mathrm{d}\omega'\mathrm{d}\Omega')$ from the infinitesimal segment of trajectory. The emissivity in the associated instantaneous rest frame with the quantum correction is then given by:

$$\Delta\alpha'(\omega', \boldsymbol{\Omega}') = \frac{e^2\omega'^2}{4\pi^2 c^3}\left|\frac{(\boldsymbol{\epsilon}'_{\mathrm{out}} \cdot \boldsymbol{\epsilon}'_{\mathrm{in}})}{\sqrt{\eta'}}\,\mathbf{v}'_{\perp}(t')\mathrm{e}^{\mathrm{i}\frac{\omega'}{\eta'}t'}\Delta t'\right|^2. \tag{10}$$

To transform this result back to the laboratory frame it is useful to note that the dot product $\boldsymbol{\epsilon}'_{\mathrm{out}} \cdot \boldsymbol{\epsilon}'_{\mathrm{in}}, \mathbf{v}'_{\perp}(t')\Delta t', \Delta\alpha'/\omega'^2$ are invariants and $\eta'(\omega', \Omega') \equiv \eta(\omega, \Omega)$, as pointed out by Lieu and Axford [28]. To facilitate the calculations, these two quantities are determined in the rest frame of the particle but expressed in terms of the variables in the lab frame [28]. The transformation of the time and frequency yields $\mathrm{i}\omega' t' = \mathrm{i}\omega(t - \mathbf{n} \cdot \mathbf{v}t/c)$ and when transforming back from the simplified reference frame to the original laboratory frame the term $\mathbf{n} \cdot \mathbf{v}t$ in the exponent yields $\mathbf{n} \cdot \mathbf{r}$.

To obtain the emissivity in the laboratory, the contributions to the total radiation spectrum from each segment $\Delta\alpha$ need to be Lorentz transformed to this frame and added coherently by summing them before taking the square of the modulus [28] in equation (10):

$$\alpha = \frac{\mathrm{d}^2 I}{\mathrm{d}\omega\mathrm{d}\,\Omega} = \frac{e^2\omega^2}{4\pi^2 c^3}\left|\int \frac{\boldsymbol{\epsilon}_{\mathrm{out}} \cdot \mathbf{v}_{\perp}}{\sqrt{\eta}}\mathrm{e}^{\mathrm{i}\frac{\omega}{\eta}(t - \mathbf{n}\cdot\mathbf{r}/c)}\mathrm{d}t\right|^2. \tag{11}$$

To facilitate the calculations, the direction of the velocity can be taken to be in the positive x direction and spherical coordinates will be used. A natural choice of unit vector in the observation direction for the outgoing radiation is then $\boldsymbol{n}' = \mathbf{e}'_{\mathbf{r}}/|\mathbf{e}'_{\mathbf{r}}|$, i.e. $\mathbf{n}' = (\cos\theta', \sin\theta'\sin\phi', \sin\theta'\cos\phi')$, where θ' is the angle between the wave vector of the outgoing radiation and the velocity and ϕ' is the angle between the two transverse components of the observation direction, z and y. The polarisation vectors can then be given by the other unit vectors in the spherical coordinates triad, $\mathbf{e}'_{\theta}$ and $\mathbf{e}'_{\phi}$, which in terms of the laboratory frame angles gives:

$$\boldsymbol{\epsilon}'^{\,1}_{\mathrm{out}} = \left(\frac{-\sin\theta}{\gamma(1 - \beta\cos\theta)}, \frac{(\cos\theta - \beta)\sin\phi}{(1 - \beta\cos\theta)}, \frac{(\cos\theta - \beta)\cos\phi}{(1 - \beta\cos\theta)}\right) \tag{12}$$

$$\boldsymbol{\epsilon}'^{\,2}_{\mathrm{out}} = (0, \cos\phi, -\sin\phi). \tag{13}$$

The displacement in the rest frame can be expressed in terms of the laboratory quantities:

$$(\Delta x', \Delta y', \Delta z') = (\gamma(v_x - v)\Delta t, v_y\Delta t, v_z\Delta t),$$

where γ is the Lorentz factor of the electron, v_x, v_y and v_z are the components of the velocity of the electron in the laboratory in the trajectory infinitesimal segment.

Substituting the rest frame displacement and the outgoing radiation polarisation vectors into equation (10) the specific emissivities in the polarisation directions $\boldsymbol{\epsilon}'^{\,\mathbf{1}}_{\mathrm{out}}$ and $\boldsymbol{\epsilon}'^{\,\mathbf{2}}_{\mathrm{out}}$, denoted by α_1 and α_2, respectively, can be computed. The two contributions can be summed inside the modulus since they are perpendicular to each other and the complete emissivity formula is obtained:

$$\frac{\mathrm{d}^2 I}{\mathrm{d}\omega\mathrm{d}\,\Omega} = \frac{e^2\omega^2}{4\pi^2 c^3}\left|\int \frac{\mathbf{n} \times (\mathbf{n} \times \boldsymbol{\beta})}{\sqrt{\eta}} \exp\left[\mathrm{i}\frac{\omega}{\eta}(t - \mathbf{n} \cdot \mathbf{r}/c)\right]\mathrm{d}t\right|^2. \tag{14}$$

This formula recovers the result of Sokolov *et al* [18], i.e. the changes in the spectrum due to recoil (neglecting spin-effect

contributions) are given by replacing the vector amplitude of emission $\mathbf{A}(\omega)$ by $(1/\sqrt{\eta})\mathbf{A}(\omega/\eta)$ in the classical emissivity formula [30]:

$$\frac{\mathrm{d}^2 I}{\mathrm{d}\omega \mathrm{d}\Omega} = \frac{e^2\omega^2}{4\pi^2 c}|\mathbf{A}(\omega)|^2 . \tag{15}$$

It also reduces to the classical emissivity in the limit $\eta \to 1$, whereas the three-dimensional result of Lieu and Axford [32] did not when $\phi \neq 0$. The emissivity obtained here is then applicable to an arbitrary observation direction. The changes in the above calculations which allowed this generalisation were two: setting the unit vector of observation direction $\mathbf{n}'$ to $\boldsymbol{n}' = \mathbf{e}'_{\mathbf{r}}/|\mathbf{e}'_{\mathbf{r}}|$ and extending the perpendicular displacement vector $\Delta\mathbf{r}' = \mathbf{v}'_{\perp}\Delta t'$ to three dimensions. We also note that in doing the integration by parts in the calculation of α_1, the term

$$\left[\frac{\exp\left(\mathrm{i}\frac{\omega}{\eta}t\right)}{\mathrm{i}\frac{\omega}{\eta}}\exp\left(-\mathrm{i}\frac{\omega}{\eta}\mathbf{n}\cdot\mathbf{r}/c\right)\right]_{-\infty}^{+\infty} \tag{16}$$

was neglected compared to

$$\int \frac{\mathbf{n}\cdot\boldsymbol{\beta}}{\sqrt{\eta}}\exp\left[\mathrm{i}\frac{\omega}{\eta}(t-\mathbf{n}\cdot\mathbf{r}/c)\right]\mathrm{d}t, \tag{17}$$

which is reasonable for sufficiently high values of ω given that $0 < \eta \leqslant 1$. Since we are interested in radiation from very relativistic particles, a significant part will be at $\omega \gg 1$. Neglecting this term facilitates the comparison of the result with the classical emissivity in the far field. However, this term can be included to deal with the lower frequencies. This has been done in JRad-QC.

It is important to stress that the only quantum effect considered here is the electron recoil, which leads to the Compton shift in the emitted frequency and the change in the scattering cross section. In the present work, the changes introduced in the radiation spectrum due to spin are not accounted for (since the Compton cross section for spinless particles is used). Although this could be overcome by considering the Compton cross section for spin-1/2 particles [28], this is expected to give a significant difference at $\chi > 1$ where the Landau and Lifshitz equation of motion will not be applicable anymore due to the increased importance of stochastic effects, pair production and emission of hard photons.

Equation (14) can be implemented in post-processing radiation diagnostic codes such as JRad [29], which is the one used in this work. The particle trajectories can be obtained from particle-in-cell codes or from the integration of the equation of motion, including the radiation reaction force.

Two considerations must be taken into account when applying this method to practical cases with the post-processing numerical tool. The first is that both the choice of time-step Δt and of the total time interval of integration affect the ranges of emitted photon frequencies that can be modelled. The maximum frequency that can be modelled is determined by the fact that there must be a sufficient number of points to resolve the photon formation time ($\Delta t \ll \tau_{\mathrm{form}}$), which is the time it takes for the radiated photon to separate itself from the electron that emits it [18, 35, 36]. For synchrotron scenarios, $\tau_{\mathrm{form}} \sim \frac{1}{\omega_L \gamma}$ [37], where ω_L is the synchrotron gyro-frequency. In the case of scattering of a laser pulse from an electron, an estimate for the photon formation time can be found from equation (21) in [18], which is of the order of $\tau_{\mathrm{form}} \sim \frac{\lambda_0}{\gamma a_0 c}$ (for $\chi \ll 1$), where λ_0 is the laser wavelength. A more general approach to obtaining the maximum frequency at which one can obtain the emissivity in a general field configuration given a set time resolution (fixed Δt) is detailed in [35].

While resolving the photon formation time leads to computationally demanding resolution requirements for PIC simulations, an alternative method has been proposed [18, 30, 35] to model the frequencies beyond the limit set above for the time-step. It uses the fact that when relativistic particles are subject to fields slowly varying in a photon formation time and linear acceleration emission can be neglected, radiation emission can be determined from the local synchrotron emissivity [18, 30, 35]. The second consideration is that the minimum frequency that can be computed with this method is such that a few photon formation times are contained in the total interaction time T given by the integration limits, i.e. the minimum frequency that can be obtained is approximately a few times γ^2/T [35].

3. Comparison with QED results obtained with a probabilistic method

As a test to the quantum corrected diagnostic (JRad-QC), the synchrotron radiation of an ultra-relativistic electron in an ultra-intense magnetic field was computed with both JRad-QC and with OSIRIS-QED [26–39]. The latter calculates the QED probability of radiation emission and determines the photon energy to be emitted using a Monte-Carlo method and the QED synchrotron radiation spectrum.

In this benchmark the spectrum of an electron with $\gamma = 200$ subject to a magnetic field of $B = 5.7 \times 10^{10}$ G (which corresponds to $\chi = 0.26$) is compared with the result from OSIRIS-QED without damping. The case without damping is presented for reference since the theoretical radiation spectrum is known, and therefore can easily be used for benchmarking purposes. In this case, the damping is turned off in OSIRIS-QED; hence the spectrum comparison tests solely whether the quantum correction in the model of Lieu and Axford reproduces the results obtained for photon production according to a QED calculation of nonlinear Compton scattering.

An analytical trajectory (without damping) was produced according to the classical equations of motion for an electron in a static magnetic field (see for example [40]). The post-processing diagnostic with quantum corrections was used to obtain the emitted spectrum as a function of a solid angle along a line perpendicular to the trajectory plane, at a distance of about 150 c/ω_r from the gyration circumference (the precise value is not relevant as long as it is in the far field), where $\omega_r = 1.88 \times 10^{15}$ rad s^{-1} is the normalisation frequency,

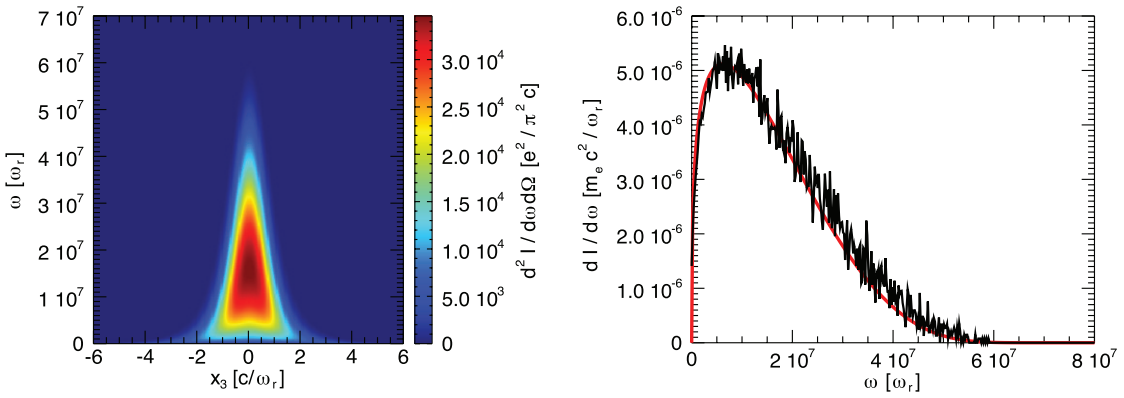

Figure 1. (Left) Spectrum determined over a line perpendicular to the synchrotron trajectory plane determined from the JRad diagnostic with quantum corrections (JRad-QC). (Right) The red line represents the synchrotron spectrum obtained with JRad-QC and the black line is the result obtained with OSIRIS-QED.

equivalent to $E = \hbar\omega_r \simeq 1.24$ eV. These spectra were then integrated into the solid angle to obtain $\mathrm{d}I/\mathrm{d}\omega$ (seen in red in figure 1). The result shows excellent agreement between the OSIRIS-QED and the JRad-QC spectra (which had been shown to be in agreement with the theoretical result for the synchrotron in the QED regime). We observe that comparisons with the QED calculations need to be done with careful consideration since the method is only valid for ultra-relativistic particles and sufficiently high fields [41–43].

4. Transition from the classical to the quantum regime

To explore the nonlinear Thomson scattering spectrum in the transition to the quantum regime, trajectories from ultra-relativistic electrons colliding with plane waves and laser pulses were produced by numerical integration of the equation of motion of Landau and Lifshitz with a Runge–Kutta method of integration of fourth order [31]. The radiation diagnostic JRad-QC / JRad was then used to compute the radiation spectra at line detectors in the far-field region with/without quantum corrections.

To investigate when quantum effects start to significantly affect the radiation spectrum a series of spectra has been computed for the case of a circularly polarised plane wave with a normalised vector potential of $a_0 = 0.88$, 1.77, 7.07 scattering off an electron with $\gamma = 10^3$ (travelling in the $+x_1$ direction) in counter-propagating geometry, which corresponds to the nonlinear quantum effects parameters of $\chi = 0.0043, 0.0086, 0.034$, respectively. The plane wave is preceded by a rising ramp but the electron energy is adjusted so that $\gamma \simeq 10^3$ at the beginning of the flat part of the wave, which lasts for $t_{\mathrm{flat}} \simeq 38\ \mathrm{T}_0 \simeq 127$ fs, where T_0 is the wave period. The virtual detector is a line at $x_3 = 0$ and the normalisation frequency is the same as the frequency of the monochromatic wave $\omega_0 = 1.88 \times 10^{15}$ rad s^{-1} (which corresponds to 1 μm wavelength or $E = \hbar\omega_0 \simeq 1.24$ eV).

Two effects are readily observed in the spectra in figure 2. First, in the case of $a_0 = 0.88$ a shift in the frequency of the harmonics can be seen. Second, in all the cases, a reduction of the radiated energy at higher frequencies is observed, as expected [14, 15]. The energy lost by the electron over the interaction time for the case of $a_0 = 7.07$ was about 21%, which gives an average energy loss rate of 0.55% per period of oscillation. This slow energy loss rate is the reason behind the almost symmetric profile in the spectra, which would not be expected if the electron were to change its energy by a significant amount during an oscillation period. It is then possible to estimate the total energy captured by the detector by doing an integration in a solid angle and in photon energy, assuming cylindrical symmetry around the direction defined by the initial momentum direction of the electron, in this example the line in the $+x_1$ direction, at $x_2 = 0$ and $x_3 = 0$. Doing so, one obtains 271 keV from the integration of the detector without quantum corrections, 104 keV for the detector with quantum corrections and 109 keV from the direct measure of the energy loss by the particle in its trajectory. The energy captured in the detector with the quantum corrections is very close to the value measured in the track, which further supports the validity of the formula for the quantum corrected emissivity.

Regarding the other values of a_0 investigated, the energy captured in the detector with quantum corrections is also closer to the energy difference measured in the track but the difference is smaller, which could be anticipated from the fact that the observed differences in the spectrum are also less significant than in the highest a_0 case.

In the scenario explored here quantum stochasticity effects have not been taken into account. It has been shown in the literature that even at $\chi < 1$ or even $\ll 1$ these effects can play a role and lead to an increased energy spread and increased spread in transverse momentum compared to the observed values in the trajectory obtained with the Landau and Lifshitz equation of motion [44, 45]. To understand the possible impact of these effects for the case of a single electron, an ensemble average of OSIRIS-QED simulations with an electron counter-propagating with a wave with the same parameters as used in the case with $a_0 = 7.07$ was performed. It was found that the estimated maximum spread in perpendicular momentum was on the order of $\Delta p_\perp \sim 2\ mc$ and in γ it was about $\Delta\gamma \sim 200$. The maximum deviation in the divergence should then be approximately $\sim(\Delta p_\perp)/ < \gamma(t_f) >$, which gives about $\sim$3 mrad, or in terms of spatial spread in our detector

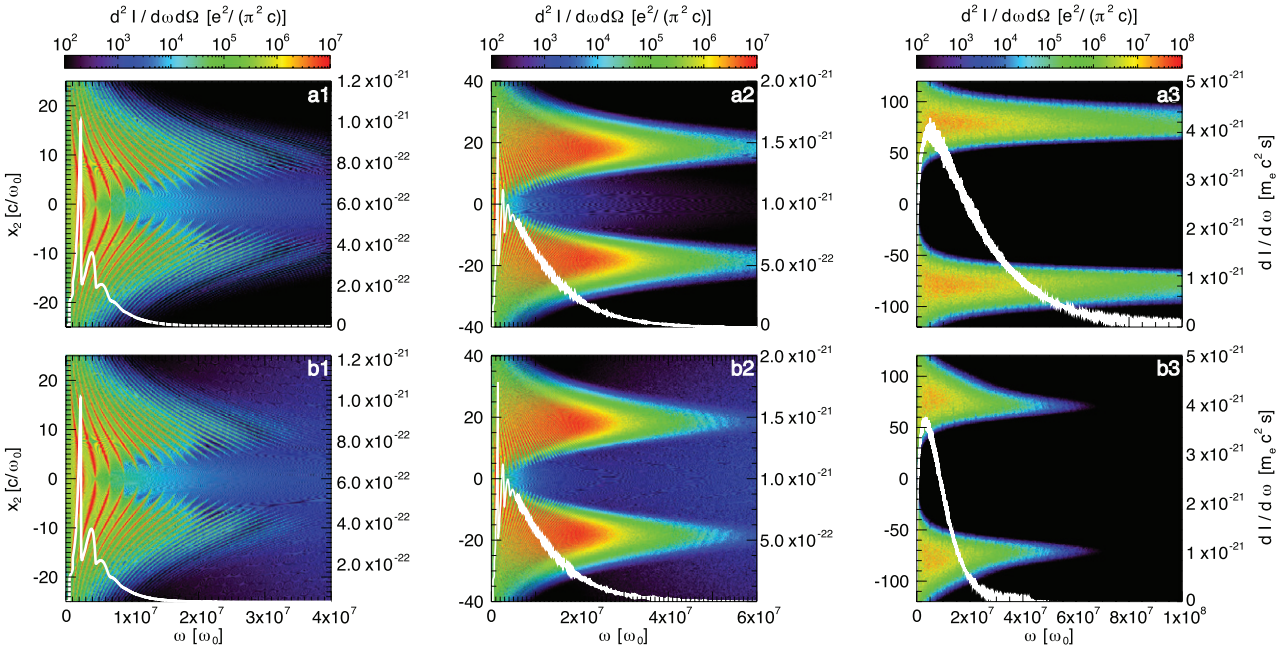

Figure 2. Spectra of the scattering of a circularly polarised plane wave with $a_0 = 0.88$ (1), $a_0 = 1.77$ (2) and $a_0 = 7.07$ (3). The plots labelled (b) refer to the calculation with quantum correction (JRad-QC) and those labelled (a) to the classical emissivity calculation (JRad). The white lines represent the spectra integrated in a solid angle assuming cylindrical symmetry.

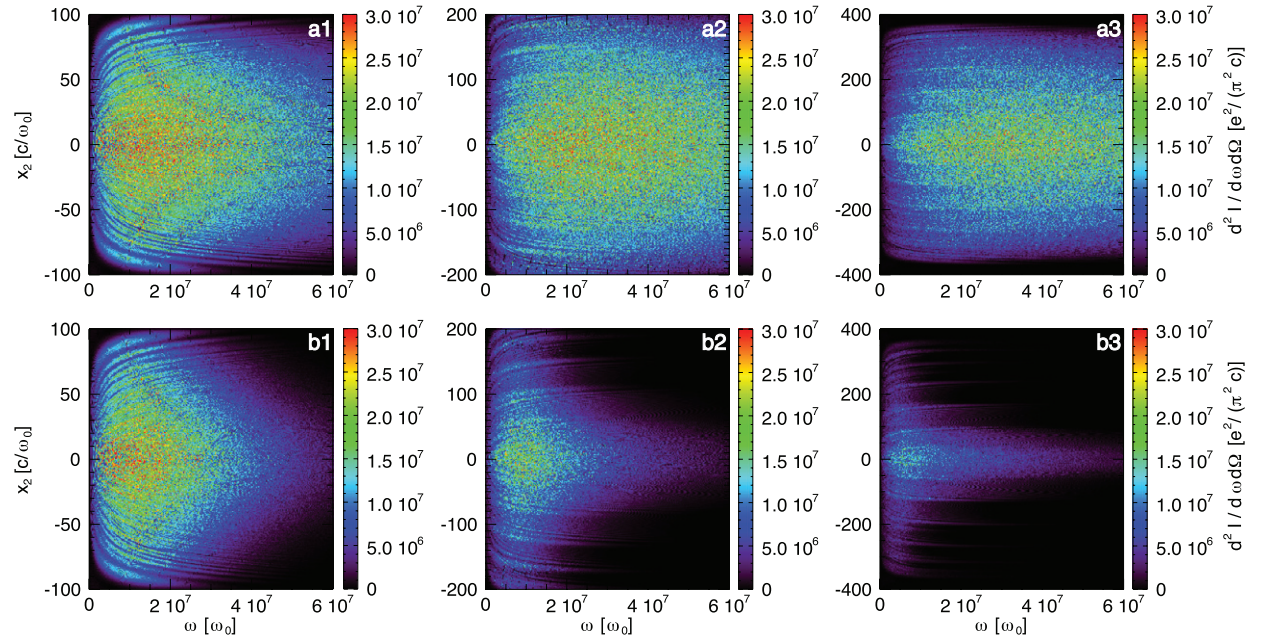

Figure 3. Spectra of the scattering of a linearly polarised laser pulse with $a_0 = 10$ (1), $a_0 = 20$ (2) and $a_0 = 30$ (3). The plots labelled (b) refer to the calculation with quantum correction (JRad-QC) and those labelled (a) to the classical emissivity calculation (JRad).

30 c/ω_0. For a more realistic beam with an initial energy and momentum spread, the analytical formulas in [44] can be used.

5. Laser pulse scattering

The scattering of a linearly polarised laser pulse from an electron with $\gamma = 1030$ (travelling in the $+x_1$ direction) in counter-propagating geometry was also explored, in a configuration similar to [4]. In the scenario studied here, the laser pulse has a 1 μm wavelength, 26.5 fs duration and a peak normalised vector potential of $a_0 = 10$, 20, 30 (corresponding to $\chi \simeq 0.035, 0.071, 0.106$ for the initial electron energy used) and is linearly polarised in the x_2 direction. The spectra computed for a line positioned at $x_1 = 10^4\ c/\omega_0$ and $x_3 = 0\ c/\omega_0$ with and without quantum corrections are depicted in figure 3. From the results, it can be seen that as the peak a_0 increases the shape of the spectrum with quantum corrections changes more and more significantly, especially at higher angles of

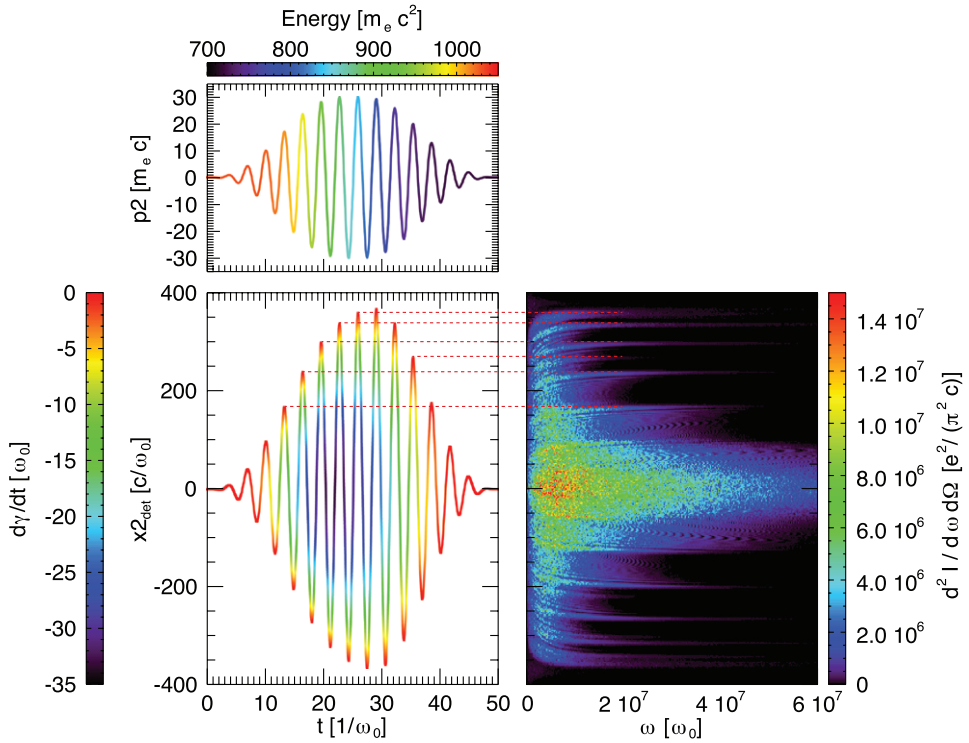

Figure 4. Evolution of the electron transverse momentum ($p2$) (top left pane) while interacting with a laser pulse with $a_0 = 30$ and of the position in the detector to which it points (bottom left pane). The line spectrum from the scattering of the laser pulse off the electron is shown (right pane). The dashed lines show the peaks in the spectrum originate from points in the trajectory where $\mathrm{d}\gamma/\mathrm{d}t = 0$, which correspond to the peaks in the transverse momentum.

observation (higher x_2 values in the detector axis). In addition, at the highest a_0 case, spike structures are clearly seen. These are correlated with the maxima in the transverse momenta, where the derivative of γ is zero (see figure 4), and also exist in the classical case. However, the quantum corrections lead to a stronger decrease in radiated energy between the spikes, making them appear more clearly.

The spectrum changes are more complex and seem more dependent in the angle in the laser pulse scattering setup compared with the plane wave scenario. This will be explored in more detail in a future publication.

As mentioned in the previous section, the calculations presented here do not include stochastic effects. These will lead to the smearing of the features observed in figure 4. Stochastic effects will in general lead to an increase in divergence and energy spread. This can counter the observed narrowing in angular interval where most of the emitted radiation is observed according to panel (b3) in figure 4. Through OSIRIS-QED simulations it was possible to estimate this effect for an electron (or a beam with zero energy and momentum spread). For the case with $a_0 = 30$ a maximum spread in momentum of the order of $\sim$6 mc and in energy of $\Delta\gamma \sim 350$ was obtained, and an estimate for the maximum change in angular angle of emission of $(\Delta p_\perp)/ < \gamma(t_f) > \sim$8 mrad which translates to $\sim$80 c/ω_0 in the spatial units of our detector. This seems to indicate that a reduction in the angular divergence of the radiation would still be observable in comparison with the purely classical calculation plotted in (a3), but for a realistic experiment a more detailed estimate of these effects needs to be undertaken accounting for the actual expected electron beam properties. The fine structures of the spectrum observed here will most likely be smeared out and not observable in that case since they are much narrower than the central part of the spectrum where most of the emitted energy is observed.

6. Conclusions

In this paper it was shown that by extending the generalised FWW method of Lieu and Axford, the emissivity with quantum corrections due to the electron recoil can be derived, which had been obtained by a different approach by Sokolov *et al* [18], through QED perturbation calculations.

The quantum corrected emissivity was implemented in the numerical diagnostic JRad [29] and was used to determine the nonlinear scattering spectrum of relativistic electrons with ultra-intense laser pulses and plane waves. It was found that only when the quantum corrections are introduced does the energy captured in the virtual detector spectrum become consistent with the energy loss by the particle (as measured from the integration of its equation of motion).

The analysis of the scattering of ultra-intense linearly polarised laser pulses from relativistic electrons revealed that the changes in the transverse momenta and energy of the electron during the interaction led to a complex spectrum shape. For larger angles of observation, spike features are observed in the spatially resolved radiation spectrum, surrounded by regions of lower radiation emission. The shape changes reflect the changes in the Compton shift during the interaction, which

were much more significant in the laser pulse scenario than in the plane wave case for the parameters used. This can be attributed to a combination of stronger radiation damping and bigger changes in the field amplitude experienced by the electron in the laser pulse scattering scenario with higher peak a_0 as compared to the plane wave cases.

Acknowledgments

This work was partially supported by the European Research Council (ERC-2010-AdG Grant 267841). The authors also wish to acknowledge the computing facilities where the simulations/post-processing were done: the SuperMUC supercomputer (through PRACE) based in the Leibniz Research Center in Germany, and the cluster ACCELERATES in the Instituto Superior Técnico in Lisbon, Portugal.

References

[1] Clayton C E *et al* 2010 *Phys. Rev. Lett.* **105** 105003
[2] Wang X *et al* 2013 *Nat. Commun.* **4** 1988
[3] Leemans W P *et al* 2014 *Phys. Rev. Lett.* **113** 245002
[4] Vranic M, Martins J L, Vieira J, Fonseca R A and Silva L O 2014 *Phys. Rev. Lett.* **113** 134801
[5] Ta Phuoc K, Corde S, Thaury C, Malka V, Tafzi A, Goddet J P, Shah R C, Sebban S and Rousse A 2012 *Nat. Photonics* **6** 308
[6] Chen S *et al* 2013 *Phys. Rev. Lett.* **110** 155003
[7] Krajewska K and Kamiński J Z 2012 *Phys. Rev.* A **85** 062102
[8] Sarachik E S and Schappert G T 1970 *Phys. Rev.* D **1** 2738
[9] Salamin Y I and Faisal F H M 1996 *Phys. Rev.* A **54** 4383
[10] Brown L S and Kibble T W B 1964 *Phys. Rev.* **133** A705
[11] Goldman I I 1964 *Sov. Phys.—JETP* **19** 954
[12] Di Piazza A, Müller C, Hatsagortsyan K Z and Keitel C H 2012 *Rev. Mod. Phys.* **84** 1117
[13] Narozhnyi N B and Fofanov M S 1996 *Sov. Phys.—JETP* **83** 14
[14] Boca M and Florescu V 2009 *Phys. Rev.* A **80** 053403
[15] Harvey C, Heinzl T and Ilderton A 2009 *Phys. Rev.* A **79** 063407
[16] Seipt D and Kämpfer B 2011 *Phys. Rev.* A **83** 022101
[17] Mackenroth F and Di Piazza A 2011 *Phys. Rev.* A **83** 032106
[18] Sokolov I V, Nees J A, Yanovsky V P, Naumova N M and Mourou G A 2010 *Phys. Rev.* E **81** 036412
[19] Thomas A G R, Ridgers C P, Bulanov S S, Griffin B J and Mangles S P D 2012 *Phys. Rev. X* **2** 041004
[20] Kirk J G, Bell A R and Arka I 2009 *Plasma Phys. Control. Fusion* **51** 085008
[21] Hartemann F V 2009 *Nucl. Instrum. Methods Phys. Res.* A **608** S1–6
[22] Chen M, Esarey E, Geddes C G R, Schroeder C B, Plateau G R, Bulanov S S, Rykovanov S and Leemans W P 2013 *Phys. Rev. ST Accel. Beams* **16** 030701
[23] Timokhin A N 2010 *Mon. Not. R. Astron. Soc.* **408** 2092–114
[24] Nerush E N, Kostyukov I Y, Fedotov A M, Narozhny N B, Elkina N V and Ruhl H 2011 *Phys. Rev. Lett.* **106** 035001
[25] Lobet M, d'Humières E, Grech M, Ruyer C, Davoine X and Gremillet L 2013 (arXiv: 1311.1107v2)
[26] Grismayer T, Vranic M, Fonseca R A, Harvey C, Ilderton A, Marklund M and Silva L O 2012 *Bull. APS* **57** 8.00076
[27] Ridgers C, Kirk J G, Duclous R, Blackburn T G, Brady C S, Bennette K, Arber T D and Bell A R 2014 *J. Comput. Phys.* **260** 273–85
[28] Lieu R and Axford W I 1993 *Astrophys. J.* **416** 700
[29] Martins J L, Martins S F, Fonseca R A and Silva L O 2009 *Proc. SPIE* **73590V** 7359
[30] Sokolov I V, Naumova N M and Nees J A 2011 *Phys. Plasmas* **18** 093109
[31] Vranic M, Martins J L, Fonseca R A and Silva L O 2015 (arXiv:1502.02432v2)
[32] Lieu R and Axford W I 1995 *Astrophys. J.* **447** 302
[33] Martins J L 2014 *PhD Thesis* Instituto Superior Técnico, Lisboa
[34] Jackson J D 1998 *Classical Electrodynamics* (New York: Wiley)
[35] Reville B and Kirk J G 2010 *Astrophys. J.* **724** 1283
[36] Akhiezer A I and Shul'ga N F 1987 *Sov. Phys.—Usp.* **30** 197
[37] Baier V N, Katkov V M and Strakhovenko V M 1998 *Electromagnetic Processes at High Energies in Oriented Single Crystals* (Singapore: World Scientific)
[38] Fonseca R A *et al* 2002 *Lecture Notes on Computer Science* vol 2331 (Berlin: Springer) p 342
[39] Vranic M, Grismayer T, Martins J, Fonseca R and Silva L 2015 *Comput. Phys. Commun.* **191** 65
[40] Rybicki G B and Lightman A P 1985 *Radiative Processes in Astrophysics* (New York: Wiley)
[41] Klepikov N P 1954 *Zh. Eksp. Teor. Fiz.* **26** 19–34
[42] Nikishov A I and Ritus V I 1967 *Sov. Phys.—JETP* **25** 1135–42
[43] Baier V N and Katkov V M 1967 *Phys. Lett.* A **25** 492–3
[44] Neitz N and Di Piazza A 2013 *Phys. Rev. Lett.* **111** 054802
[45] Green D G and Harvey C N 2014 *Phys. Rev. Lett.* **112** 164801